



**HAL**  
open science

## Functional interactions of the SPAK/OSR1 kinases with their upstream activator WNK1 and downstream substrate NKCC1

Alberto C Vitari, Jacob Thastrup, Fatema Rafiqi, Maria Deak, Nick A Morrice, Håkan Kr Karlsson, Dario R Alessi

### ► To cite this version:

Alberto C Vitari, Jacob Thastrup, Fatema Rafiqi, Maria Deak, Nick A Morrice, et al.. Functional interactions of the SPAK/OSR1 kinases with their upstream activator WNK1 and downstream substrate NKCC1. *Biochemical Journal*, 2006, 397 (1), pp.223-231. 10.1042/BJ20060220 . hal-00478531

**HAL Id: hal-00478531**

**<https://hal.science/hal-00478531>**

Submitted on 30 Apr 2010

**HAL** is a multi-disciplinary open access archive for the deposit and dissemination of scientific research documents, whether they are published or not. The documents may come from teaching and research institutions in France or abroad, or from public or private research centers.

L'archive ouverte pluridisciplinaire **HAL**, est destinée au dépôt et à la diffusion de documents scientifiques de niveau recherche, publiés ou non, émanant des établissements d'enseignement et de recherche français ou étrangers, des laboratoires publics ou privés.

**Functional interactions of the SPAK/OSR1 kinases with their upstream activator WNK1 and downstream substrate NKCC1.**

Alberto C. Vitari<sup>1</sup>, Jacob Thastrup<sup>1</sup>, Fatema Rafiqi<sup>1</sup>, Maria Deak<sup>1</sup>, Nick A. Morrice<sup>1</sup>, Håkan K. R. Karlsson<sup>1</sup> and Dario R. Alessi<sup>1</sup>

MRC Protein Phosphorylation Unit<sup>1</sup>, School of Life Sciences, MSI/WTB complex, University of Dundee, Dow Street, Dundee DD1 5EH, Scotland.

Correspondence to: ACV ([a.c.vitari@dundee.ac.uk](mailto:a.c.vitari@dundee.ac.uk)).

Tel 01382 384241 Fax 01382 223778

Running Title: Interactions of SPAK/OSR1 with WNK1 and NKCC1.

**Abbreviations:** CATCHtide, CATion CHloride cotransporter SPAK/OSR1 peptide substrate; CCT domain, Conserved C-Terminal domain of SPAK/OSR1; GST, Glutathione-S-Transferase; KCC, K-Cl-Cotransporter; NCC, Na-Cl-Cotransporter; NKCC, Na-K-Cl-Cotransporter; OSR1, Oxidative Stress Response kinase-1; SD, Standard Deviation; SPAK, STE20/SPS1-related Proline-Alanine-rich Kinase; WNK, With-No-K(lysine) protein kinase.

**Key words:** pseudohypoaldosteronism type II; Gordon's syndrome; cation cotransporters; hypertension, protein kinase.

**Abstract.** The STE20/SPS1-related Proline-Alanine-rich Kinase (SPAK) and Oxidative Stress Response kinase-1 (OSR1) kinases interact and phosphorylate the Na-K-Cl cotransporter-1 (NKCC1), leading to its activation. Recent studies indicated that SPAK and OSR1 are phosphorylated and activated by the WNK1 (With-No-K(Lys) protein kinase-1) and WNK4, genes mutated in humans affected by Gordon's hypertension syndrome. Here we identify 3 residues in NKCC1 (Thr175/Thr179/Thr184-shark or Thr203/Thr207/Thr212-human), that are phosphorylated by SPAK and OSR1, and develop a peptide substrate (CATCHtide), to assess SPAK and OSR1 activity. Exposure of 293 cells to osmotic stress, which leads to phosphorylation and activation of NKCC1, increased phosphorylation of NKCC1 at the sites targeted by SPAK/OSR1. The residues on NKCC1, phosphorylated by SPAK/OSR1, are conserved in other cation cotransporters, such as the NaCl cotransporter, the target of thiazide drugs that lower blood pressure in humans with Gordon's syndrome. Furthermore, we characterise the properties of a 92 residue Conserved C-Terminal (CCT) domain on SPAK and OSR1 that interacts with an RFXV motif present in the substrate NKCC1 and its activators WNK1/WNK4. A peptide containing the RFXV motif interacts with nanomolar affinity with the CCT domains of SPAK/OSR1, and can be utilised to affinity purify SPAK and OSR1 from cell extracts. Mutation of the Arg, Phe or Val within this peptide abolishes binding to SPAK/OSR1. We identify specific residues within the CCT required for interaction with the RFXV motif and demonstrate that mutation of these in OSR1 inhibited phosphorylation of NKCC1, but not of the CATCHtide peptide that does not possess an RFXV motif. We establish that an intact CCT domain is required for WNK1 to efficiently phosphorylate and activate OSR1. These data establish that the CCT domain functions as a multi-purpose docking-site, enabling SPAK/OSR1 to interact with substrates (NKCC1) and activators (WNK1/WNK4).

## Introduction.

The STE20/SPS1-related Proline-Alanine-rich Kinase (SPAK) and Oxidative Stress Response kinase-1 (OSR1) protein kinases were originally identified through their ability to interact with and stimulate the activity of the Na-K-Cl cotransporter (NKCC1) [1, 2]. SPAK and OSR1 are 68% identical in sequence, possess a highly similar kinase catalytic domain as well as a Conserved C-Terminal (CCT) domain, comprising 92 amino acids that are 79% identical in sequence. The CCT domain interacts with Arg-Phe-Xaa-Val motifs in NKCC1 [1] as well as other potential binding partners [3, 4]. Recent studies indicate that the WNK1 [With No K (lysine) protein kinase-1] and WNK4 enzymes phosphorylate and activate the SPAK and OSR1 protein kinases [5, 6]. Mutations in the genes encoding WNK1 and WNK4 enzymes are found in families with an inherited hypertension and hyperkalemia (elevated plasma K<sup>+</sup>) disorder termed Gordon's Syndrome or Pseudohypoaldosteronism type II [7]. The WNK1 and WNK4 protein kinases phosphorylate SPAK and OSR1 at their T-loop residue (Thr233-SPAK, Thr185-OSR1) in addition to a non-catalytic Ser residue lying in a conserved motif between the catalytic and CCT domains (Ser373-SPAK, Ser325-OSR1) [6]. Mutational analysis indicates that phosphorylation of the T-loop in SPAK and OSR1 rather than the phosphorylation of the Ser residue mediates activation by WNK1 [6]. Consistent with this, mutation of the T-loop Thr, phosphorylated by WNK1/WNK4, to a Glu residue to mimic phosphorylation increases the basal activity of OSR1 [6] and SPAK (ACV unpublished results) over 10-fold and prevents further activation by WNK1. In this study, we map the residues on NKCC1 that are phosphorylated by the SPAK and OSR1 kinases and we show that endogenous NKCC1 phosphorylation at these sites is increased in response to hyperosmotic stress in cells. Furthermore, we develop a peptide substrate that can be employed to easily assess the activity of these kinases. We also characterise the binding properties of the CCT domain and establish that it plays an important role in regulating the activation of SPAK/OSR1 by WNK1 as well as the phosphorylation of SPAK and OSR1 substrates such as NKCC1.

## Materials and Methods.

**Materials.** Sequencing-grade trypsin and protease-inhibitor cocktail tablets were from Roche; dialysed fetal-bovine serum and other tissue-culture reagents were from Life Technologies; [ $\gamma$ <sup>32</sup>P]ATP, streptavidin Sepharose High performance and glutathione-Sepharose 4B were from Amersham Biosciences; Colloidal Blue Staining Kit from Invitrogen. Tween-20 was from Sigma. Nonidet P40 was from Fluka; P81 phosphocellulose paper was from Whatman. GST-PreScission Protease was expressed and purified from *E. coli* using plasmids kindly provided by Professor

John Heath (School of Biosciences, University of Birmingham, Edgbaston, Birmingham, U.K.) and Professor David Barford (Institute of Cancer Research, Chester Beatty Laboratories, Fulham, London, U.K.). All peptides were synthesised by Dr Graham Bloomberg (Molecular Recognition Centre, University of Bristol School of Medical Sciences, Bristol, U.K.). Sensor chips SA were from BiaCore AB (Stevenage, UK).

**General methods, buffers and DNA construct.** Tissue culture, transfection, immunoblotting, restriction-enzyme digests, DNA ligations and other recombinant DNA procedures were performed using standard protocols. All mutagenesis were carried out using the QuikChange Site-Directed Mutagenesis system (Stratagene) using the KOD polymerase (Novagen). DNA constructs used for transfection were purified from *E. coli* DH5 $\alpha$  using Qiagen plasmid Mega or Maxi kit according to the manufacturer's protocol. All DNA constructs were verified by DNA sequencing, which was performed by The Sequencing Service, School of Life Sciences, University of Dundee, Scotland, U.K., using DYEnamic ET terminator chemistry (Amersham Biosciences) on Applied Biosystems automated DNA sequencers. Lysis Buffer was 50 mM Tris/HCl, pH 7.5, 1 mM EDTA, 1 mM EGTA, 1% (w/w) Nonidet P40, 1 mM sodium orthovanadate, 50 mM NaF, 5 mM sodium pyrophosphate, 0.27 M sucrose, 1 mM DTT (dithiothreitol) and Complete protease inhibitor cocktail (one tablet per 50 ml). Buffer A was 50 mM Tris/HCl, pH 7.5, 0.1 mM EGTA and 1 mM DTT. Sample Buffer was 1X NuPAGE<sup>®</sup> LDS sample buffer (Invitrogen) containing 1% (by vol)  $\beta$ -mercaptoethanol. For expression of proteins in *E.coli*, pGEX-6P-1 constructs were transformed into BL21 *E. coli* cells, expressed and purified as described previously [6]. For expression of proteins in 293 cells this was undertaken as described previously [6]. The cloning of human WNK1 [8], SPAK, OSR1 and a fragment corresponding to amino acid residues 1-260 of dogfish shark NKCC1 [6] were described previously.

**Mapping phosphorylation sites on NKCC1.** The activation assay mixtures were set up in a total volume of 25  $\mu$ l of Buffer A, containing 0.25  $\mu$ M GST-WNK1[1-661] (expressed in *E.coli*), 5 $\mu$ M GST-SPAK or 5 $\mu$ M GST-OSR1 (expressed in *E.coli*), 10 mM MgCl<sub>2</sub> and 0.1 mM non-radioactive ATP. After incubation for 40 min at 30°C, 5  $\mu$ l of the activation assay mix was transferred to 20  $\mu$ l of Buffer A containing 6.25  $\mu$ M NKCC1[1-260] expressed in *E.coli*, 10 mM MgCl<sub>2</sub> and 0.1 mM [ $\gamma$ -<sup>32</sup>P]ATP (~3000 cpm/pmol). After incubation for 40 min at 30°C, incorporation of phosphate was determined following electrophoresis of samples on a NuPAGE<sup>®</sup> Bis-Tris 10% gels and autoradiography of Coomassie-stained gels. The proteins band corresponding to NKCC1 was excised and phosphate incorporation was quantified on a Perkin Elmer liquid scintillation analyzer. Following tryptic digestion more than >87% of the

<sup>32</sup>P-radioactivity incorporated in the gel bands was recovered and the samples were chromatographed on a reverse phase HPLC Vydac 218TP5215 C<sub>18</sub> column (Separations Group, Hesperia, CA, U.S.A.) as described in the legend of Figure 1. Fractions corresponding to the major <sup>32</sup>P-containing peaks were analysed using an Applied Biosystems 4700 Proteomics Analyzer (MALDI-TOF/TOF) and solid-phase Edman degradation on an Applied Biosystems 494C sequenator of the peptide coupled to Sequelon-AA membrane (Milligen Corp., Bedford, MA, U.S.A.) [9].

**In vitro NKCC1 phosphorylation reactions.** Assays were set up in a total volume of 25  $\mu$ l of Buffer A containing 1  $\mu$ M GST-OSR1[T185E] or GST-SPAK[T233E] expressed in *E. coli*, 5  $\mu$ M NKCC1[1-260], GST-NKCC1[1-260] or GST-NKCC1[1-260/T175A/T179A/T184A], 10 mM MgCl<sub>2</sub> and 0.1 mM [ $\gamma$ -<sup>32</sup>P]ATP (~300 cpm/pmol). After incubation for 40 min at 30°C, incorporation of phosphate was determined as described above.

**OSR1 kinase assays employing CATCHtide or NKCC1[1-260].** Assays were set up in a total volume of either 50  $\mu$ l (CATCHtide assay) or 25  $\mu$ l (NKCC1 assay) in Buffer A containing 10 mM MgCl<sub>2</sub>, 0.1 mM [ $\gamma$ -<sup>32</sup>P]ATP (~300 cpm/pmol), 0.08-0.5  $\mu$ M of GST-OSR1[T185E] 300  $\mu$ M CATCHtide (RRHYYYDTHNTYYLRTFGHNTRR) or 5  $\mu$ M NKCC1[1-260]. After incubation for 10-60 min at 30 °C, the reaction mixture was applied onto P81 phosphocellulose paper, the papers washed in phosphoric acid and incorporation of <sup>32</sup>P-radioactivity in CATCHtide was quantified as described previously [10]. For the NKCC1 assay the reaction was stopped by the addition of SDS sample Buffer and phosphorylation of NKCC1 assessed as described above following SDS-PAGE.

**Antibodies.** For immunoblotting of WNK1, an antibody raised in sheep against WNK1 protein encompassing residues 61-661 expressed in *E. coli* was utilised [8]. For the immunoprecipitation of WNK1 (Fig 8), we employed an antibody raised against a C-terminal (residues 2360-2382 of human WNK1, QNFNISNLQKSISNPPGSNLRTT) [8]. For immunoblotting of phosphorylated NKCC1 (Fig 2) an antibody raised in sheep against a peptide encompassing residues 198-217 of human NKCC1 phosphorylated at Thr203, Thr207 and Thr212 was utilized (HYYYDT(P)HTNT(P)YYLRT(P)FGHNT). For the immunoprecipitation and immunoblotting of NKCC1 from 293 cells in Figure 2B, an antibody raised in sheep against shark NKCC1[1-260] expressed and purified from *E. coli* was utilized. T4 anti-NKCC1 mouse monoclonal antibody was purchased from Developmental Studies Hybridoma Bank (Iowa University, Iowa City) and used for immunoblotting of NKCC1 in Figures 4 and 5. Mouse monoclonal antibodies recognizing glutathione S-transferase were purchased from Sigma (#G1160). Secondary antibodies coupled to fluorophores were from Molecular Probes and Rockland.

**Immunoblotting.** Samples were heated in sample buffer, subjected to SDS/PAGE and transferred to nitrocellulose. Membranes were blocked for 5 min in TBST [50 mM Tris/HCl (pH 7.5)/0.15 M NaCl/0.2% Tween-20], containing 10 % (w/v) skimmed milk. The membranes were then incubated for 16 h at 4°C in TBST containing 10 % (w/v) skimmed with 0.5 µg/ml of the WNK1 antibody, 2 µg/ml of the phospho-NKCC1 antibody, 5 µg/ml of the NKCC1[1-260] antibody or 10000-fold dilution for GST antibody or 100 µg/ml of ascites containing monoclonal T4 anti-NKCC1 antibody. Detection was performed using fluorophores conjugated antibody and Li-Cor Odyssey® infrared imaging system.

**Affinity purification of SPAK and OSR1 employing the biotin-RFQV peptide.** 1 mg clarified 293 cell lysate expressing forms of GST-OSR1 (Fig 6B) or 10 mg of untransfected 293 cell lysate (Fig 6D) was incubated with 3 µg of the indicated biotinylated peptide for 15 min at 4°C. 10 µl Streptavidin beads equilibrated in Lysis Buffer were added. After 15min incubation at 4°C under gentle agitation, the beads were washed 2 times with Lysis Buffer containing 0.5M NaCl followed by 2 washes with Buffer A. The beads were boiled in 1X NuPAGE® LDS sample buffer and the samples were subjected to SDS/PAGE. The gels were either transferred to nitrocellulose for immunoblotting or stained with Colloidal Blue Staining Kit according to manufactures protocol and processed for MS fingerprinting.

**Immunoprecipitation of endogenous WNK1 and NKCC1.** 293 cells grown on 10 cm diameter dishes were lysed in 0.5 ml of Lysis Buffer and clarified by centrifugation at 14,000 x g for 5 min. For immunoprecipitations, 0.5 mg (WNK1) or 2 mg (NKCC1) of lysate were incubated at 4 °C for 1 h with 5 µL of protein G Sepharose beads conjugated to 5 µg of anti WNK1-(C-terminus) antibody, 1.5 µg of anti NKCC1[1-260] antibody or the equivalent amount of pre immune antibody. The immunoprecipitates were washed twice with Lysis Buffer containing 0.5M NaCl, and twice with Buffer A.

**Biacore analysis.** Binding was analysed in a BiaCore 3000 system (BiaCore AB, Stevenage, UK). The indicated biotinylated peptides were bound to a streptavidin-coated Sensor chip (SA) (400 response units, RU). The indicated concentrations of bacterially expressed wild type and mutant forms of GST-OSR1 fusion protein in HBS-EP buffer (10 mM HEPES pH 7.4, 0.15 M NaCl, 3 mM EDTA, 0.005% (v/v) polysorbate-20), were injected over the immobilised peptides at a flow rate of 30 µl/min. Interactions between each peptide and the GST-OSR1 forms were analysed and steady state binding was determined at each concentration. Dissociation of GST-OSR1 forms from each peptide was monitored over 90 sec. Regeneration of the Sensor chip surface between each injection was performed with 3 consecutive 5-µl injections of a solution containing 10 mM NaOH and 1 M NaCl.

## Results.

**Mapping residues in NKCC1 that are phosphorylated by SPAK and OSR1.** To define the residues in the N-terminal regulatory domain of NKCC1 that are phosphorylated by SPAK and OSR1, we employed a fragment of shark NKCC1 encompassing residues 1-260, that SPAK and OSR1 are known to phosphorylate efficiently [2, 5, 6]. Under the conditions employed, NKCC1[1-260] was phosphorylated by active SPAK or OSR1 to ~0.15 mol of phosphate/mol, digested with trypsin and chromatographed on a C<sub>18</sub> column to isolate <sup>32</sup>P-labelled phosphopeptides (Fig 1A & 1B). Both profiles were similar revealing the presence of two major phosphopeptides termed P1 and P2. Mass spectroscopy and Edman sequencing established the identity of P1 as a doubly phosphorylated peptide at Thr175 and Thr179 (corresponding to Thr203, Thr207 in human NKCC1, Fig 3A) and P2 as a peptide phosphorylated at Thr184 (corresponding to Thr212 in human NKCC1, Fig 3A). We next assessed how mutation of these residues affected the phosphorylation of NKCC1[1-260]. Individual mutation of Thr175, Thr179 or Thr184 to Ala, moderately reduced phosphorylation of NKCC1 by SPAK (Fig 1C) and OSR1 (Fig 1D), whilst a mutant of NKCC1 in which all three residues were changed to Ala, was not longer phosphorylated by either SPAK (Fig 1C) or OSR1 (Fig 1D).

**Phosphorylation of endogenous NKCC1.** In order to study whether endogenous NKCC1 was phosphorylated on the residues that are phosphorylated by SPAK/OSR1, we raised a phosphospecific antibody against a peptide encompassing residues 198-217 of human NKCC1 phosphorylated on Thr203, Thr207 and Thr212. This antibody recognised NKCC1[1-260] only after it was phosphorylated by active OSR1 in vitro (Fig 2A). A mutant form of NKCC1[1-260], in which Thr203, Th207 and Thr212 were changed to Ala, was not recognised by the phospho-NKCC1 antibody after incubation with active OSR1 and MgATP (Fig 2A). We next assessed whether endogenous NKCC1 was phosphorylated at the residues targetted by SPAK and OSR1. Previous work demonstrated that hyperosmotic stress such as sorbitol induces hyperphosphorylation and activation of NKCC1 [11]. To verify whether sorbitol increased phosphorylation of endogenous NKCC1 at the sites phosphorylated by SPAK and OSR1, we treated 293 cells in the presence or absence of 0.5 M sorbitol and immunoblotted cell lysates or NKCC1 immunoprecipitates with the phospho-NKCC1 antibody. These data demonstrate that sorbitol increased phosphorylation of NKCC1 by 2-fold (Fig 2B).

**Generation of a peptide substrate for SPAK and OSR1.** A peptide encompassing residues 198 to 217 of human NKCC1 (almost identical to residues 170 to 189 of shark NKCC1, see Fig 3A) in which two Arg residues were added to the N and C-termini to increase solubility and ability to interact with phosphocellulose-p81 paper

was generated. This peptide was phosphorylated by the active OSR1[T185E] mutant with a  $K_m$  of 330  $\mu$ M and a  $V_{max}$  of 5.7 U/mg (Fig 3B). Similar results were obtained using the active SPAK[T233E] mutant (ACV data not shown). This peptide was termed CATion-CHloride cotransporter-peptide (CATCHtide), and can be employed to assess SPAK/OSR1 activity in a facile manner, using the assay described in the Materials and Methods.

**Residues of CCT domain of SPAK and OSR1 required for binding to NKCC1 and WNK1.** Previous studies with yeast 2-hybrid analysis indicated that the Conserved C-Terminal (CCT) domain of SPAK and OSR1 bound to NKCC1 [1] as well as WNK4 [3, 4], through an Arg-Phe-Xaa-Val motif (where Xaa is any amino acid). Consistent with this, we found that full length SPAK or OSR1 or the isolated CCT domain of these enzymes, when expressed in 293 cells, interacted with endogenously expressed NKCC1 (Fig 4A). We were unable to detect endogenously expressed WNK4 in 293 cells, but found that endogenously expressed WNK1 that possesses five Arg-Phe-Xaa-Val motifs, interacted with the CCT containing fragments of SPAK and OSR1 (Fig 4A). Mutant forms of SPAK and OSR1 lacking the CCT domain failed to bind NKCC1 or WNK1 (Fig 4A). To determine which residues on the CCT domain were required for interaction with NKCC1 and WNK1, we undertook an alanine-scan in which we investigated the effect of mutating 46 residues in CCT domain on its ability to bind to endogenously expressed NKCC1 and WNK1. Most mutations did not affect the binding, however a few including Asp479 and Leu493 disrupted binding of the SPAK-CCT domain to both WNK1 and NKCC1 (Fig 4B). We also observed that mutations of other residues namely Thr480, Val484, Glu487, Val494, Asp498, Val502 affected binding to NKCC1 to a greater extent than WNK1.

**CCT domain of OSR1 is required for efficient phosphorylation of NKCC1.** To verify whether removal of the CCT domain affected the intrinsic catalytic activity of OSR1, we first assayed this enzyme with the CATCHtide peptide, which does not possess an Arg-Phe-Xaa-Val motif, and would therefore not be expected to interact directly with the CCT domain. Both full length OSR1[T185E] and a mutant of OSR1 lacking the CCT domain (OSR1[T185E]- $\Delta$ CCT), phosphorylated CATCHtide with similar efficiency (Fig 5A), indicating that removal of the CCT domain does not affect the intrinsic OSR1 catalytic activity. We next tested the efficiency with which the OSR1[T185E]- $\Delta$ CCT mutant phosphorylated NKCC1, and observed that it was only able to phosphorylate NKCC1[1-260] at low background level, similar to that observed with an inactive OSR1[T185A] mutant. We also investigated how mutations in the CCT domain affected the ability of full length OSR1 expressed in 293 cells to interact with NKCC1 and WNK1 (Fig 5B). Consistent with the results of the isolated

CCT domain, the full length OSR1[T185E/D459A], OSR1[T185E/V464A] and OSR1[T185E/L473A] mutants failed to interact with endogenously expressed WNK1 and NKCC1 under conditions in which wild type OSR1 and OSR1[T185E] bound strongly (Fig 5B). Moreover, the OSR1[T185E/D459A], OSR1[T185E/V464A] and OSR1[T185E/L473A] mutants that failed to interact with NKCC1 only phosphorylated NKCC1[1-260] poorly, while they retained normal catalytic activity towards the CATCHtide peptide substrate (Fig 5B).

**Characterisation of binding properties of the CCT domain.** In order to analyse the properties of the CCT domain in more detail, we synthesised a biotinylated peptide that encompasses the Arg-Phe-Xaa-Val motif on WNK4, proposed to mediate the interaction with SPAK [3]. We investigated the ability of this peptide to interact with wild type and mutant forms of OSR1, deploying a quantitative BiaCore surface plasmon resonance binding assay. The isolated OSR1 CCT domain interacted with the Arg-Phe-Gln-Val motif containing peptide with high affinity (apparent  $K_d$  of 8 nM, Fig 6A). Several of the CCT domain mutants tested including OSR1[D459A], OSR1[V464A] and OSR1[L473A] as well as OSR1- $\Delta$ CCT, failed to bind the Arg-Phe-Gln-Val peptide. Other mutants (OSR1[V474A], OSR1[T460A]) interacted with the Arg-Phe-Gln-Val peptide with lower affinity than the wild type CCT domain (Fig 6A). Similar results were obtained when binding of the Arg-Phe-Gln-Val peptide to these mutants was assessed in a 293-cell lysate peptide pull down assay (Fig 6B). We next studied how mutation of the Arg-Phe-Gln-Val motif affected binding of the peptide to the CCT domain. The Ala-Phe-Gln-Val, Arg-Ala-Gln-Val and Arg-Phe-Gln-Ala peptides failed to bind the OSR1 CCT domain, whilst the Arg-Phe-Ala-Val peptide bound to this domain with similar affinity as the parental Arg-Phe-Gln-Val peptide (Fig 6C). Employing the biotinylated Arg-Phe-Gln-Val or Arg-Phe-Ala-Val peptides coupled to streptavidin-Sepharose, we were able to affinity purify sufficient amounts of endogenously expressed SPAK and OSR1 from 10 mg of 293 cell lysate to visualise on a coomassie stained gel and identify by mass spectrometry (Fig 6D). In contrast, we were unable to affinity purify SPAK and OSR1 using the non SPAK/OSR1-binding peptides (Fig 6D).

The Arg-Phe-Gln-Val peptide did not affect the ability of OSR1[T185E] to phosphorylate CATCHtide (Fig 7A), indicating that interaction of the CCT domain with an interacting partner does not directly stimulate kinase activity. In contrast, the Arg-Phe-Gln-Val peptide suppressed in a dose-dependent manner phosphorylation of NKCC1[1-260] by OSR1[T185E], further establishing the necessity of the CCT domain in enabling OSR1 to phosphorylate NKCC1 (Fig 7A). Consistent with this, peptides that are unable to bind the CCT domain did not suppress phosphorylation of NKCC1[1-260] by OSR1[T185E] (Fig 7B).

**The CCT domain facilitates activation of OSR1 by WNK1.** We next studied how removal of the CCT domain of OSR1 affected its phosphorylation (Fig 8A) and activation (Fig 8B) by full length WNK1 in vitro. We compared the ability of endogenous WNK1, immunoprecipitated from 293 cell lysates, to phosphorylate full length OSR1 or OSR1- $\Delta$ CCT. WNK1 phosphorylated full length OSR1 more efficiently than the OSR1- $\Delta$ CCT mutant lacking the CCT domain (Fig 8A). In addition, we found that endogenously expressed WNK1 immunoprecipitated from 293 cells activated full length OSR1 30-fold over a 40 min period (Fig 8B). In contrast, the OSR1- $\Delta$ CCT mutant was only activated ~10-fold in a parallel experiment (Fig 8B).

### Discussion.

It is well established that phosphorylation of the N-terminal intracellular regulatory domain of NKCC1 plays a crucial role in regulating the activity of this cation co-transporter [11, 12]. In vivo  $^{32}$ P-labelling experiments of shark rectal gland tubules identified 3 phosphorylation sites on NKCC1 (Thr184, Thr 189 and Thr202), that were stimulated with forskolin and calyculin-A [13]. Mutation of Thr189, but not Thr184 and Thr202 was found to inhibit activation of NKCC1 [13]. Another more recent study indicated that the individual mutation of the equivalent sites on rabbit NKCC2 did not significantly affect cotransporter activity, but mutation of all three residues markedly inhibited activity [14]. SPAK and OSR1 were originally identified as kinases that interacted with and activated NKCC1 [1, 4]. Further evidence that SPAK regulates the activity of NKCC1 came from the finding that overexpression of dominant negative SPAK inhibited NKCC1 phosphorylation and activation [2]. Direct mapping of the residues on NKCC1 that are phosphorylated by SPAK and OSR1 has not previously been undertaken. Here we demonstrate that SPAK and OSR1 phosphorylate a cluster of 3 residues on shark NKCC1 (Thr175, Thr179 and Thr184) and that mutation of all 3 sites is required to prevent phosphorylation of NKCC1 by SPAK and OSR1 (Fig 1). Importantly, we also establish that sorbitol stimulation of cells, which is known to lead to phosphorylation and activation of NKCC1 [11], increases the phosphorylation of NKCC1 at the residues targeted by SPAK and OSR1 in vitro (Fig 2B). Further work will be required to assess the effect that mutation of Thr175, Thr179 and Thr184 has on NKCC1 activity in unstimulated and osmotically stressed cells. In addition, it would be important to establish how inhibition of SPAK/OSR1 and WNK isoforms affects activation and phosphorylation of NKCC1 at the Thr175, Thr179 and Thr184 residues. As mentioned above, only the effect of mutating Thr184 of NKCC1, has previously been investigated, and its mutation did not substantially affect NKCC1 activity [13, 14]. It is therefore possible

that phosphorylation of Thr175 and Thr179 in addition to Thr184, contribute to activation of NKCC1 by SPAK and OSR1, and this will need to be verified by further experimentation. Our peptide mapping studies indicate that Thr189 and Thr202 on NKCC1 are not phosphorylated by SPAK and OSR1 *in vitro*, suggesting that other protein kinase(s) are likely to be targeting those sites *in vivo*.

The residues in NKCC1 phosphorylated by SPAK and OSR1 as well as the residues surrounding them, are conserved in NKCC2 and the Na-Cl cotransporter (NCC, Fig 3A). NCC is the target of the thiazide drugs which effectively lower blood pressure in patients with Gordon's syndrome [7, 15]. The WNK1 kinase is reportedly overexpressed in humans with mutations in the intronic non-coding region of the WNK1 gene, indicating that overexpression of WNK1 results in hypertension [7]. Consistent with this notion, heterozygous WNK1<sup>-/+</sup> mice have lower blood pressure [16]. It would be interesting to investigate the activity of the SPAK/OSR1 kinases, as well as the activity and phosphorylation of NKCC1/2 and NCC in patients with Gordon's syndrome and WNK1<sup>-/+</sup> mice. The SPAK and OSR1 phosphorylation sites are not conserved on any of the isoforms of the K-Cl Cotransporter (KCC) family (Fig 3A), suggesting that they may not be controlled in the same manner by SPAK/OSR1. However, KCC3, but not KCC1, KCC2 and KCC4, possesses a putative CCT-binding Arg-Phe-Met-Val motif in a similar position as found in NKCC1/2 and NCC and therefore may explain why KCC3 was found to interact with SPAK/OSR1 in a yeast 2 hybrid screen [1]. It would be interesting to investigate whether SPAK/OSR1 are capable of phosphorylating and regulating the activity of KCC3.

Our results are consistent with previous studies [1, 3, 4] indicating that the CCT domain of SPAK and OSR1 interacts with Arg-Phe-Xaa-Val motifs on NKCC1 as well as WNK1 and WNK4 with high affinity. However, our work does not exclude the possibility that variants of the Arg-Phe-Xaa-Val motif might also interact with the CCT domain. It would be of interest to undertake binding analysis employing peptide arrays, in which each of the residues within the Arg-Phe-Xaa-Val motif was mutated to all of the other amino acids. Our work also defines for the first time, a number of mutations in the CCT domain that specifically abolish interaction with NKCC and WNK1. It would be informative to crystallise the CCT domain to define the molecular mechanism by which this domain binds the Arg-Phe-Xaa-Val motif with high affinity. Our findings in this study demonstrate for the first time that a functional CCT domain is essential for efficient binding and phosphorylation of the NKCC1 substrate by SPAK and OSR1, but not the CATCHtide peptide substrate which does not possess an Arg-Phe-Xaa-Val motif. These results indicate that the CCT domain functions as a specific substrate recognition domain, which enables

docking of Arg-Phe-Xaa-Val motif containing substrates and hence their efficient phosphorylation by SPAK and OSR1. Our results also support the notion that the CCT domain is required for efficient phosphorylation and activation of OSR1 by WNK1, as we observe that the OSR1 mutant lacking the CCT domain is markedly less phosphorylated and activated by full length WNK1 than the wild type OSR1 (Fig 8).

Many kinases such as MAP kinases, GSK3 and PDK1 rely on substrate recognition sites termed docking-sites that recognise motifs on their substrate distant from the sites that are phosphorylated (reviewed in [17]). In MAP kinases, GSK3 and PDK1, the substrate docking regions are located within a specific pocket of the catalytic domain itself. In contrast, SPAK and OSR1 have evolved a specific relatively large 92-residue domain separate from the kinase domain to interact with substrates as well as upstream regulators. Further work is required to explore how the CCT domain interaction with WNK1 or NKCC1 is coordinated in a manner that permits SPAK/OSR1 to become first activated by WNK1/WNK4 and subsequently interact with their substrates. It would also be interesting to determine whether SPAK and OSR1 interact with substrates other than NKCC or other cotransporters through their CCT domain.

**Acknowledgements.** We thank Steven L. Roberds (Pfizer St Louis) for support, Gursant Kular for help with the Biacore analysis, David Campbell for mass spectrometry analysis, Agnieszka Kieloch and Gail Fraser for technical assistance, the Sequencing Service (School of Life Sciences, University of Dundee, Scotland) for DNA sequencing, the Post Genomics and Molecular Interactions Centre for Mass Spectrometry facilities (School of Life Sciences, University of Dundee, Scotland) and the protein production and antibody purification teams [Division of Signal Transduction Therapy (DSTT), University of Dundee] co-ordinated by Hilary McLauchlan and James Hastie for expression and purification of antibodies. ACV is the recipient of Pfizer sponsored studentship. HKRK is supported by a long term FEBS fellowship. DRA is supported by the Association for International Cancer Research, Diabetes UK, the Medical Research Council, the Moffat Charitable Trust and as well as the pharmaceutical companies that support the DSTT (AstraZeneca, Boehringer-Ingelheim, GlaxoSmithKline, Merck & Co. Inc, Merck KGaA and Pfizer).

## References

- 1 Piechotta, K., Lu, J. and Delpire, E. (2002) Cation chloride cotransporters interact with the stress-related kinases Ste20-related proline-alanine-rich kinase (SPAK) and oxidative stress response 1 (OSR1). *J. Biol. Chem.* **277**, 50812-50819
- 2 Dowd, B. F. and Forbush, B. (2003) PASK (proline-alanine-rich STE20-related kinase), a regulatory kinase of the Na-K-Cl cotransporter (NKCC1). *J. Biol. Chem.* **278**, 27347-27353
- 3 Gagnon, K. B., England, R. and Delpire, E. (2005) Volume sensitivity of cation-chloride cotransporters is modulated by the interaction of two kinases: SPAK and WNK4. *Am. J. Physiol. Cell Physiol.*
- 4 Piechotta, K., Garbarini, N., England, R. and Delpire, E. (2003) Characterization of the interaction of the stress kinase SPAK with the Na<sup>+</sup>-K<sup>+</sup>-2Cl<sup>-</sup> cotransporter in the nervous system: evidence for a scaffolding role of the kinase. *J. Biol. Chem.* **278**, 52848-52856
- 5 Moriguchi, T., Urushiyama, S., Hisamoto, N., Iemura, S., Uchida, S., Natsume, T., Matsumoto, K. and Shibuya, H. (2005) WNK1 regulates phosphorylation of cation-chloride-coupled cotransporters via the STE20-related kinases, SPAK and OSR1. *J. Biol. Chem.* **280**, 42685-42693
- 6 Vitari, A. C., Deak, M., Morrice, N. A. and Alessi, D. R. (2005) The WNK1 and WNK4 protein kinases that are mutated in Gordon's hypertension syndrome, phosphorylate and activate SPAK and OSR1 protein kinases. *Biochem. J.*
- 7 Wilson, F. H., Disse-Nicodeme, S., Choate, K. A., Ishikawa, K., Nelson-Williams, C., Desitter, I., Gunel, M., Milford, D. V., Lipkin, G. W., Achard, J. M., Feely, M. P., Dussol, B., Berland, Y., Unwin, R. J., Mayan, H., Simon, D. B., Farfel, Z., Jeunemaitre, X. and Lifton, R. P. (2001) Human hypertension caused by mutations in WNK kinases. *Science* **293**, 1107-1112
- 8 Vitari, A. C., Deak, M., Collins, B. J., Morrice, N., Prescott, A. R., Phelan, A., Humphreys, S. and Alessi, D. R. (2004) WNK1, the kinase mutated in an inherited high-blood-pressure syndrome, is a novel PKB (protein kinase B)/Akt substrate. *Biochem. J.* **378**, 257-268
- 9 Campbell, D. G. and Morrice, N. A. (2002) Identification of Protein Phosphorylation Sites by a Combination of Mass Spectrometry and Solid Phase Edman Sequencing. *J. Biomol. Techn.* **13**, 121-132
- 10 Alessi, D. R., Cohen, P., Ashworth, A., Cowley, S., Leever, S. J. and Marshall, C. J. (1995) Assay and expression of mitogen-activated protein kinase, MAP kinase kinase, and Raf. *Methods Enzymol.* **255**, 279-290
- 11 Lytle, C. and Forbush, B., 3rd (1992) The Na-K-Cl cotransport protein of shark rectal gland. II. Regulation by direct phosphorylation. *J. Biol. Chem.* **267**, 25438-25443
- 12 Kurihara, K., Moore-Hoon, M. L., Saitoh, M. and Turner, R. J. (1999) Characterization of a phosphorylation event resulting in upregulation of the salivary Na<sup>(+)</sup>-K<sup>(+)</sup>-2Cl<sup>(-)</sup> cotransporter. *Am. J. Physiol.* **277**, C1184-1193
- 13 Darman, R. B. and Forbush, B. (2002) A regulatory locus of phosphorylation in the N terminus of the Na-K-Cl cotransporter, NKCC1. *J. Biol. Chem.* **277**, 37542-37550
- 14 Gimenez, I. and Forbush, B. (2005) Regulatory phosphorylation sites in the NH2 terminus of the renal Na-K-Cl cotransporter (NKCC2). *Am. J. Physiol. Renal Physiol.* **289**, F1341-1345

- 15 Gordon, R. D. and Hodsman, G. P. (1986) The syndrome of hypertension and hyperkalaemia without renal failure: long term correction by thiazide diuretic. *Scott. Med. J.* **31**, 43-44
- 16 Zambrowicz, B. P., Abuin, A., Ramirez-Solis, R., Richter, L. J., Piggott, J., BeltrandelRio, H., Buxton, E. C., Edwards, J., Finch, R. A., Friddle, C. J., Gupta, A., Hansen, G., Hu, Y., Huang, W., Jaing, C., Key, B. W., Jr., Kipp, P., Kohlhauff, B., Ma, Z. Q., Markesich, D., Payne, R., Potter, D. G., Qian, N., Shaw, J., Schrick, J., Shi, Z. Z., Sparks, M. J., Van Sligtenhorst, I., Vogel, P., Walke, W., Xu, N., Zhu, Q., Person, C. and Sands, A. T. (2003) Wnk1 kinase deficiency lowers blood pressure in mice: a gene-trap screen to identify potential targets for therapeutic intervention. *Proc. Natl. Acad. Sci. U S A* **100**, 14109-14114
- 17 Biondi, R. M. and Nebreda, A. R. (2003) Signalling specificity of Ser/Thr protein kinases through docking site-mediated interactions. *Biochem. J.* **372**, 1-13
- 18 Rice, P., Longden, I. and Bleasby, A. (2000) EMBOSS: the European Molecular Biology Open Software Suite. *Trends Genet.* **16**, 276-277

**Figure legends.**

**Figure 1. Sites on NKCC1 phosphorylated by SPAK and OSR1.** (A) Shark NKCC1[1-260] was phosphorylated by wild type SPAK as described in the Materials and Methods. The  $^{32}\text{P}$ -labelled NKCC1 was isolated by electrophoresis on a polyacrylamide gel, digested with trypsin and the resulting peptides were chromatographed on a  $\text{C}_{18}$  column equilibrated in 0.1% (v/v) trifluoroacetic acid in water. The column was developed with a linear acetonitrile gradient (diagonal line) at a flow rate of 0.2 ml/min and fractions of 0.1 ml were collected. The peak fractions containing the major  $^{32}\text{P}$ -labelled peptides are marked as P1 and P2. The indicated peptides were analysed by MALDI TOF–TOF mass spectrometry as described in the Materials and Methods. The site of phosphorylation within each peptide was determined by solid phase Edman sequencing in which  $^{32}\text{P}$ -radioactivity was measured after each cycle of Edman degradation. The cycle number in which  $^{32}\text{P}$ -radioactivity was released is indicated. The deduced amino acid sequences of P1 and P2 are indicated in which the phosphorylated residues are underlined. (B) As above, except that wild type OSR1 was employed in place of SPAK. (C) Active SPAK[T233E] was incubated with bacterially expressed wild type NKCC1[1-260] or the indicated mutants in the presence of  $\text{Mg}[\gamma\text{-}^{32}\text{P}]\text{ATP}$ . After incubation, the samples were analysed by polyacrylamide gel electrophoresis and phosphorylation of NKCC1 protein substrate was determined by scintillation counting. Abbreviation NKCC1-TTTAAA corresponds to a mutant in which Thr175, Thr179 and Thr184 were all mutated to Ala. (D) As above, except that active OSR1[T185E] was employed in place of SPAK[T233E].

**Figure 2. Phosphorylation of endogenous NKCC1.** (A) The indicated forms of GST-NKCC1[1-260] were incubated with or without constitutively active OSR1[T185E] in presence of MgATP and immunoblotted with phospho-NKCC1 antibody (p-NKCC1) or an anti-GST antibody. (B) 293 cells were incubated with or without 0.5 M sorbitol for 30 min and then lysed. Cell lysates (40  $\mu\text{g}$ ), or immunoprecipitations undertaken from 2 mg of lysate with NKCC1 or pre-immune IgG, were analysed by immunoblotting with the phospho-NKCC1 or an antibody raised against NKCC1[1-260]. Similar results were obtained in 3 separate experiments. Quantification of the phospho-NKCC1 immunoblot was undertaken using the Li-Cor Odessey infrared imaging system. Results are presented relative to the mean value observed in unstimulated cells, which was given a value of 1.0. Abbreviations: OSR1[T185E], GST-OSR1[T185E]; GST-NKCC1 wt, GST-NKCC1[1-260]; GST-NKCC1[TTTAAA], GST-NKCC1[1-260/T175A/T179A/T184A].

**Figure 3. Generation of a peptide substrate for OSR1.** (A) Multiple sequence alignment of the indicated fragments of cation chloride cotransporters encompassing the NKCC1 SPAK and OSR1 sites of phosphorylation, performed using the program T-Coffee [18]. The alignment was graphically represented with BOXSHADE version 3.21 at [http://www.ch.embnet.org/software/BOX\\_form.html](http://www.ch.embnet.org/software/BOX_form.html) using standard parameters. Identical residues are highlighted in black and similar residues in grey. The region of NKCC1 that encompasses the CATCHtide peptide is marked with a solid line, the sites phosphorylated by SPAK and OSR1 are marked with a triangle and the previously identified residues on NKCC1 phosphorylated in cells [13] are marked with squares. Abbreviations: hNKCC1, human NKCC1 and sNKCC1, shark NKCC1. (B) Constitutively active GST-OSR1[T185E] was incubated with the indicated amount of CATCHtide in presence of Mg[ $\gamma^{32}$ P]ATP and incorporation of  $^{32}$ P-phosphate into the substrate determined. Each assay was carried out in triplicate and the results are presented as the mean  $\pm$  SD. Similar results were obtained in at least 3 experiments.

**Figure 4. Analysis of interaction of SPAK and OSR1 with WNK1 and NKCC1.** (A) 293 cells were transfected with constructs encoding the indicated GST-fusion proteins. 36 h post transfection, the GST-fusion proteins were affinity purified on glutathione-Sepharose beads that were immunoblotted with GST, WNK1 or NKCC1 antibody to detect endogenously associated WNK1 and NKCC1. Abbreviations SPAK wt, GST-SPAK[full length 1-547]; SPAK NT, GST-SPAK[1-455]; SPAK CCT, GST-SPAK[449-547]; OSR1 wt, GST-OSR1[full length 1-527]; OSR1 NT, GST-OSR1[1-435]; OSR1 CCT, GST-OSR1[429-527]. (B) 293 cells were transfected with constructs encoding the isolated CCT domain of SPAK (GST-SPAK[449-547]) or the mutants in which the indicated residues had been mutated to an Ala. Binding of NKCC1 and WNK1 to these was assessed as above. Residues marked with an asterisk represent mutations that markedly affected binding to NKCC1 and/or WNK1, whilst residues marked with a square although they affected binding to NKCC1 and WNK1 were also found to markedly decrease expression of the isolated CCT domain as well as the full length protein (data not shown).

**Figure 5. Role of the CCT domain in enabling OSR1 to phosphorylate NKCC1 and CATCHtide.** (A & B) 293 cells were transfected with constructs encoding the indicated mutants of OSR1 as GST-fusion proteins. 36 h post transfection, the fusion proteins were affinity purified and incubated with CATCHtide (upper graph) or sNKCC1[1-260] (lower graph) as substrates in the presence of Mg[ $\gamma^{32}$ P]ATP and phosphorylation of these substrates was determined as described in Material and

Methods. The results are presented relative to the kinase activity observed with GST-OSR1[T185E], which was given a value of 100. The purified GST-OSR1 proteins were also immunoblotted with indicated antibodies. Abbreviations TA, GST-OSR1[T185A]; TE, GST-OSR1[T185E]; TA/ $\Delta$ CCT, GST-OSR1[T185A/ $\Delta$ CCT/residues 1-435]; TE/ $\Delta$ CCT, GST-OSR1[T185E/ $\Delta$ CCT/residues 1-435]; TE/CCT[DA], GST-OSR1[T185E/D459A]; TE/CCT[VA], GST-OSR1[T185E/V464A]; TE/CCT[LA], GST-OSR1[T185E/L473A]; wt, GST-OSR1; TE, GST-OSR1[T185E].

**Figure 6. Analysis of binding properties of the CCT domain.** (A) The binding of bacterially expressed isolated forms of the OSR1 CCT domain (residues 429-527) or OSR1- $\Delta$ CTT (residues 1-435) to a biotinylated RFQV containing peptide derived from WNK4 (biotin-SEEGKPQLVGRFQVTSSK) was analysed using BiaCore as described in Materials and Methods. The analysis was performed over a range of protein concentration (6.8-340 nM) and the response level at steady-state was plotted against the log of the protein concentration. The  $K_D$ 's were calculated by fitting the data to the formula ( $Y=B_{max} * X / (K_D + X)$ ) using GraphPad 4 software, which describes the binding of a ligand to a receptor that follows the law of mass action.  $B_{max}$  is the maximal binding and  $K_D$  is the concentration of ligand required to reach half-maximal binding. Whereas X and Y correspond to the protein concentration and the response units respectively. The insert shows the similar level of the recombinant proteins employed for this analysis. (B) 293 cells were transfected with GST tagged wild type OSR1 or the indicated mutants. 36 h post transfection, cell were lysed and subjected to affinity purification with the biotinylated RFQV peptide as described in the materials and methods. The affinity purified samples (termed pull down) were immunoblotted with an anti-GST antibody to detect interaction of GST-fusion proteins with the peptide. The cell lysates prior to affinity purification (termed input) were also subjected to immunoblotting. (C) As in (A) except that binding of the isolated OSR1 CTT domain to the indicated biotinylated peptides was determined. The peptide sequences employed are RFQV, biotin-SEEGKPQLVGRFQVTSSK; AFQV, biotin-SEEGKPQLVGAFQVTSSK; RAQV, biotin-SEEGKPQLVGRAQVTSSK; RFAV, biotin-SEEGKPQLVGRFAVTSSK; RFQA, biotin-SEEGKPQLVGRFQATSSK. (D) Non-transfected 293 cell lysates were incubated with the biotinylated peptides described in (C) and subjected to affinity purification with Streptavidin-Sepharose. The purified samples were analysed on a Coomassie stained SDS/PAGE gel. The bands marked with an asterisk were subjected to MS fingerprinting and their identity confirmed as endogenously expressed SPAK and OSR1.

**Figure 7. Effect of RFQVtide on OSR1 kinase activity.** (A) GST-OSR1[T185E] was incubated with either NKCC1[1-260] (5  $\mu$ M) or CATCHtide (10  $\mu$ M) or alone in the presence of Mg[ $\gamma^{32}$ P]ATP and the indicated concentration of RFQV peptide. After incubation the phosphorylation of substrates was determined. The results are the mean  $\pm$  SD of a triplicate experiment. Similar results were obtained in 2 separate experiments. (B) As above except that samples were incubated with the 1 mM of the indicated peptides whose sequence is same as described in the legend to Fig 6, except that they were not biotinylated.

**Figure 8. Role of the CCT domain in regulating OSR1 activation by WNK1.** (A) WNK1 immunoprecipitated from 293 cell lysate (filled symbols) or a control immunoprecipitation performed with pre-immune IgG (Pre-Imm IgG) antibody (open symbols), was incubated in the presence of Mg[ $\gamma^{32}$ P]ATP and the indicated concentration of full length kinase inactive OSR1[ki] or kinase inactive OSR1[ki- $\Delta$ CCT] purified from *E.coli*. After incubation phosphorylation of the OSR1 substrate was determined and results are presented as the mean of a duplicate experiment  $\pm$  SD. The insert shows a Coomassie stained SDS/PAGE of the purified proteins quantified using Li-Cor Odyssey<sup>®</sup> infrared imaging system to ensure that a similar molar concentration of full length OSR1[ki] and mutant OSR1[ki- $\Delta$ CCT] were employed in the assay. Abbreviations: OSR1[ki], full length OSR1[D164A] (residues 1-527); OSR1[ki- $\Delta$ CCT]; OSR1[1-435/D164A] (OSR1- $\Delta$ CCT, that lacks the CCT domain, residues 1-435). (B) Full length GST-OSR1 or GST-OSR1- $\Delta$ CCT purified from *E.coli* were incubated with either WNK1 immunoprecipitated from 293-cell lysate (filled symbols) or with a control immunoprecipitation performed with pre immune IgG antibody (open symbols), in the presence of CATCHtide substrate and Mg[ $\gamma^{32}$ P]ATP. After the indicated time of incubation phosphorylation of the CATCHtide substrate was determined and results are presented as activity for the mean of a triplicate experiment  $\pm$  SD. The insert shows a Coomassie stained SDS/PAGE of the purified GST-fusion proteins quantified using Li-Cor Odyssey<sup>®</sup> infrared imaging system to ensure that a similar molar concentration of wild type OSR1 and mutant OSR1- $\Delta$ CCT were employed in the activity assay. Recombinant OSR1 migrates as a doublet band with upper band migrating with the expected molecular mass. We presume that the lower band is a proteolytic fragment containing the kinase domain and lacking the C-terminal portion as these enzymes were expressed as N-terminal GST fusion proteins. Abbreviations: OSR1-wt, wild type GST-OSR1; OSR1- $\Delta$ CCT, GST-OSR1[1-435].

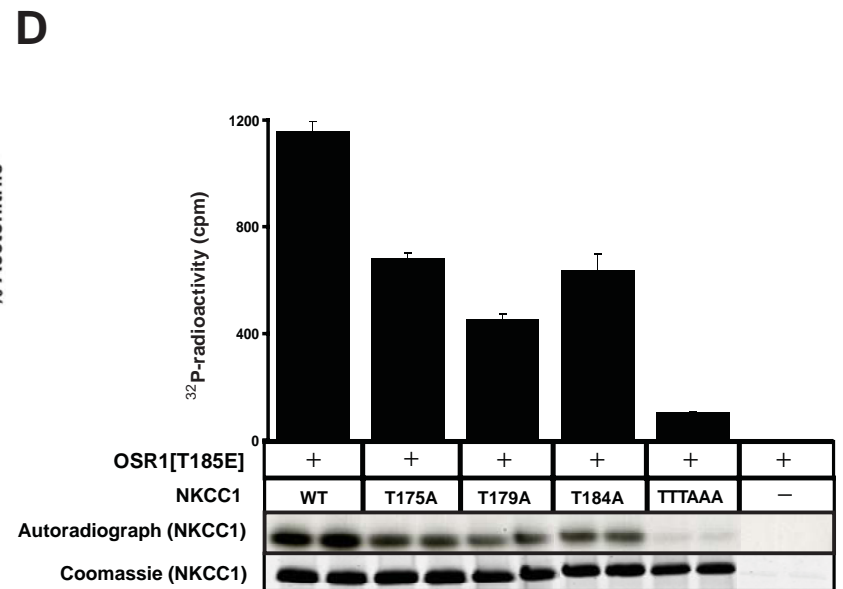
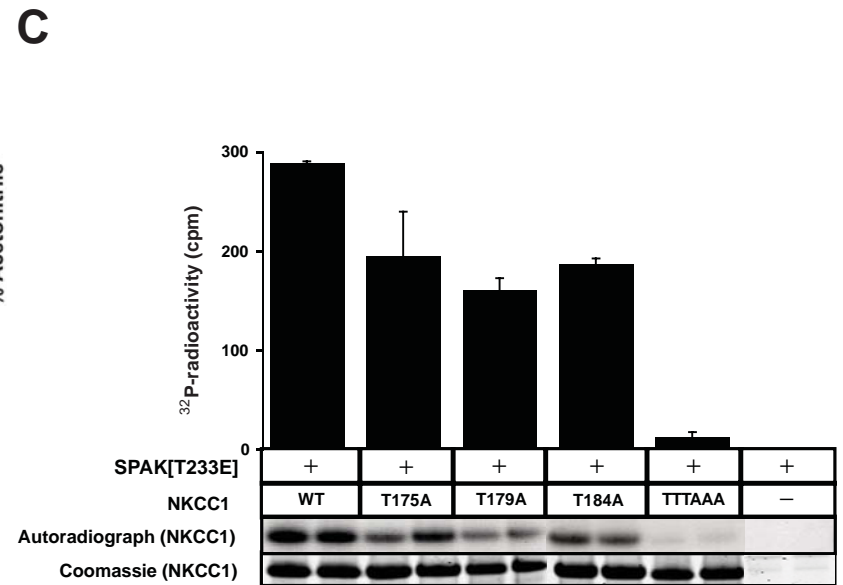
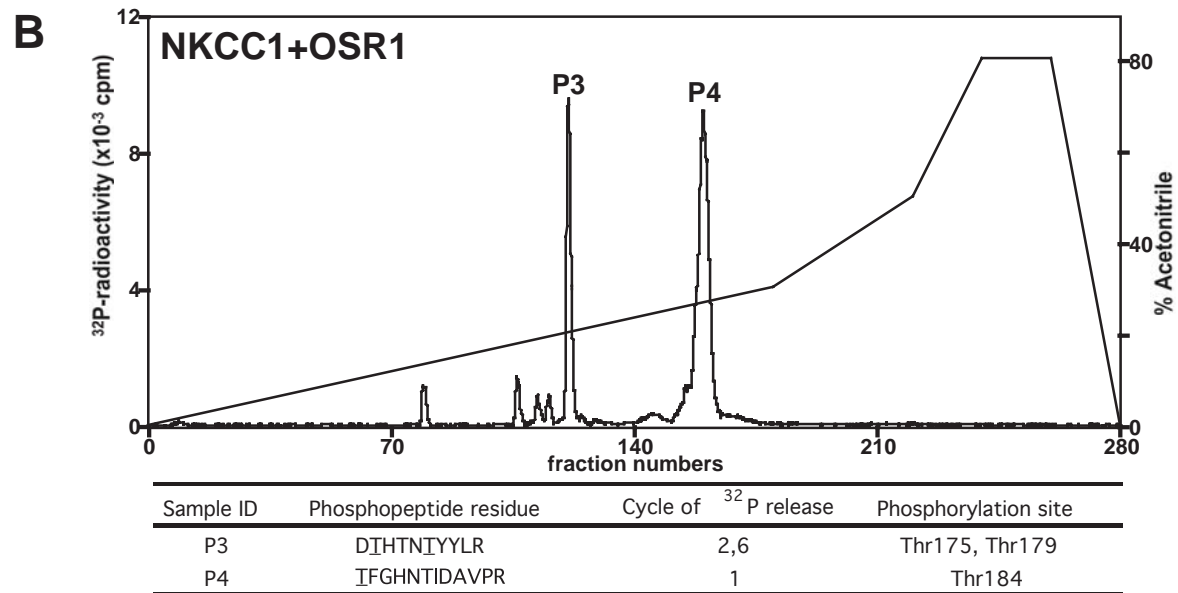
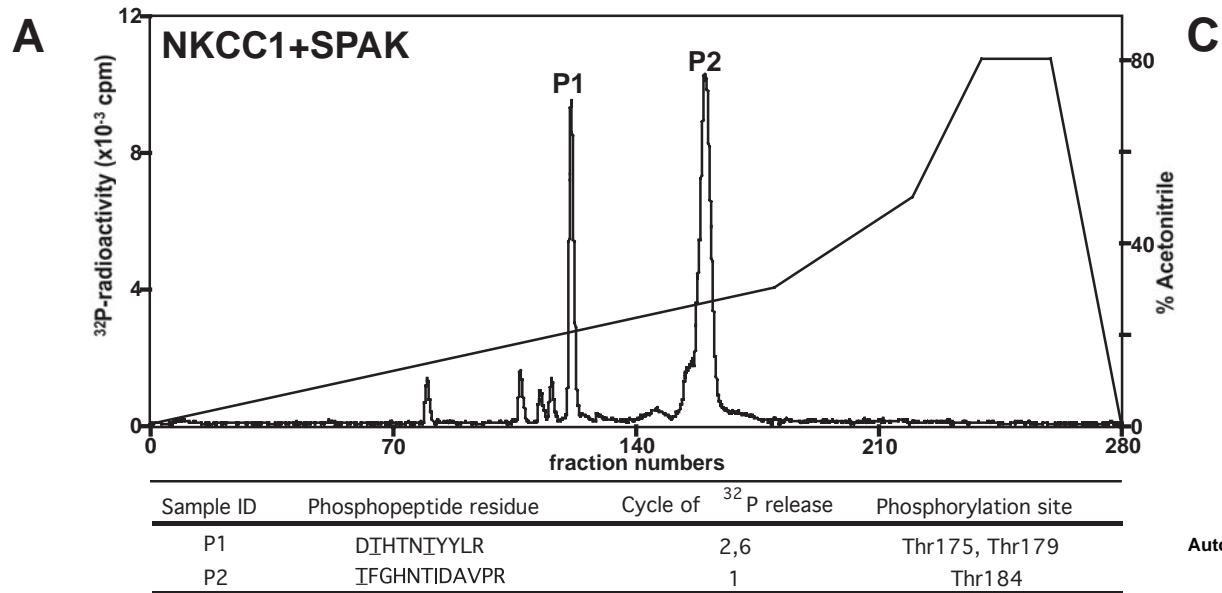
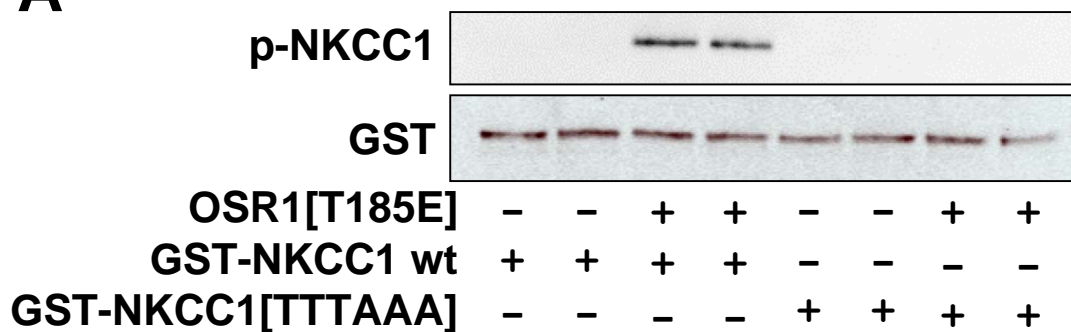
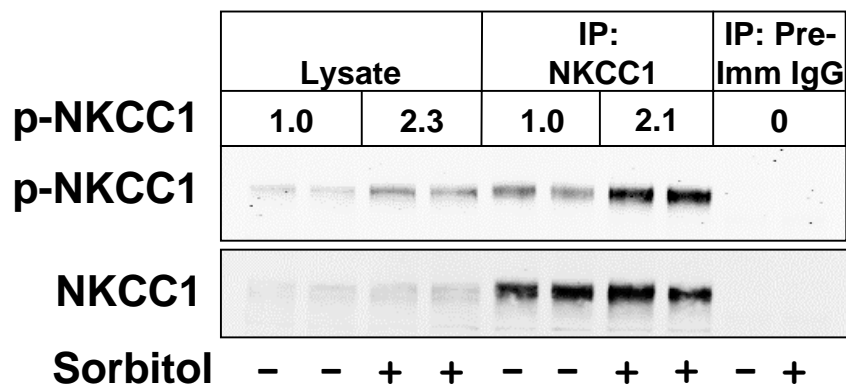


Fig1

**A**



**B**



**Fig 2**

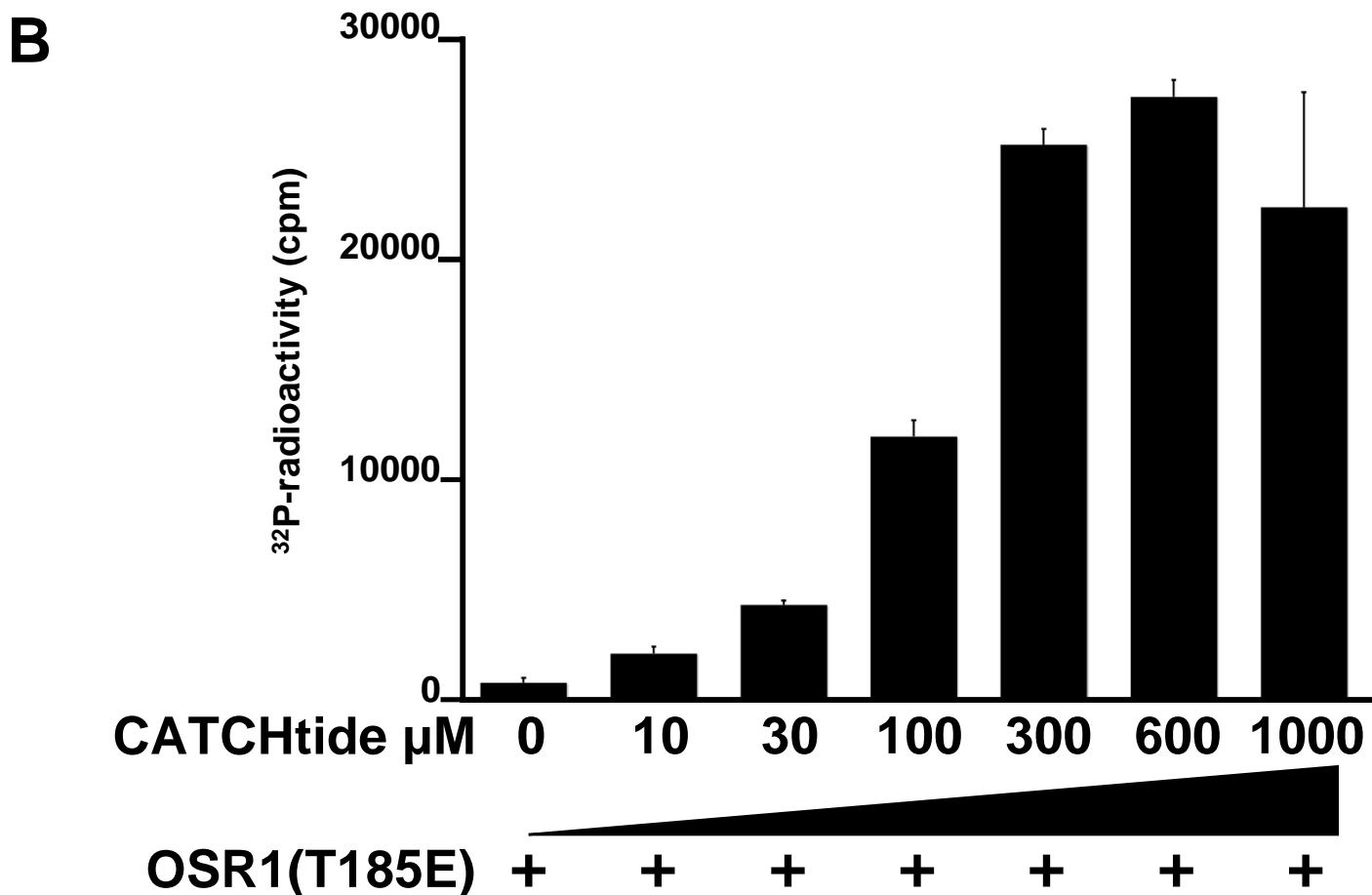
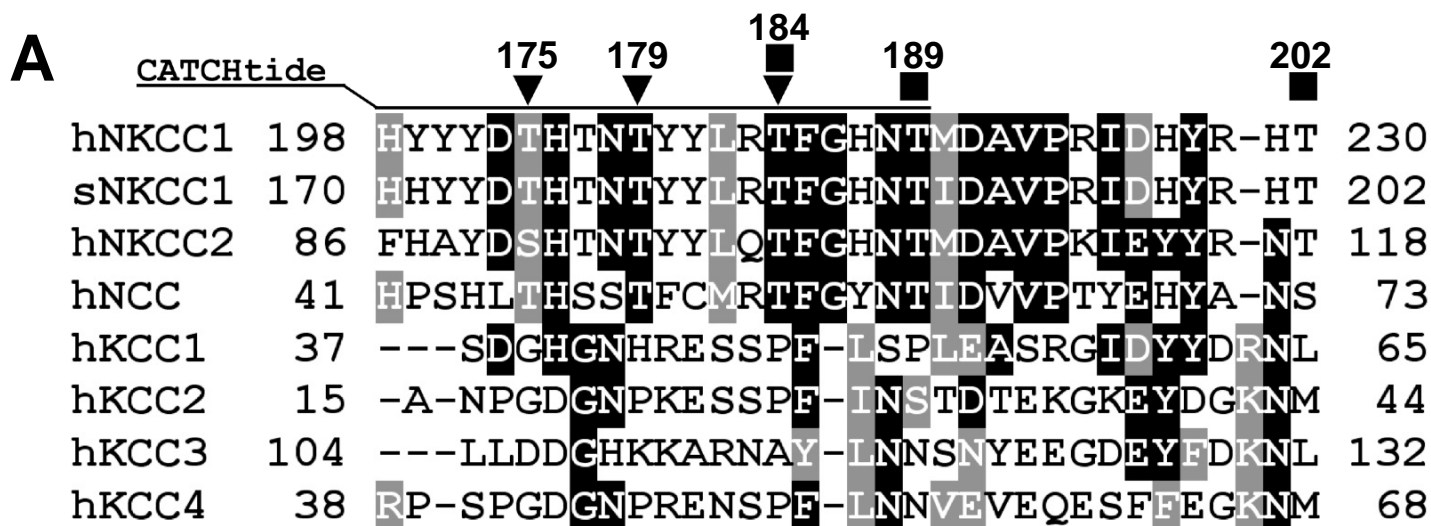


fig3

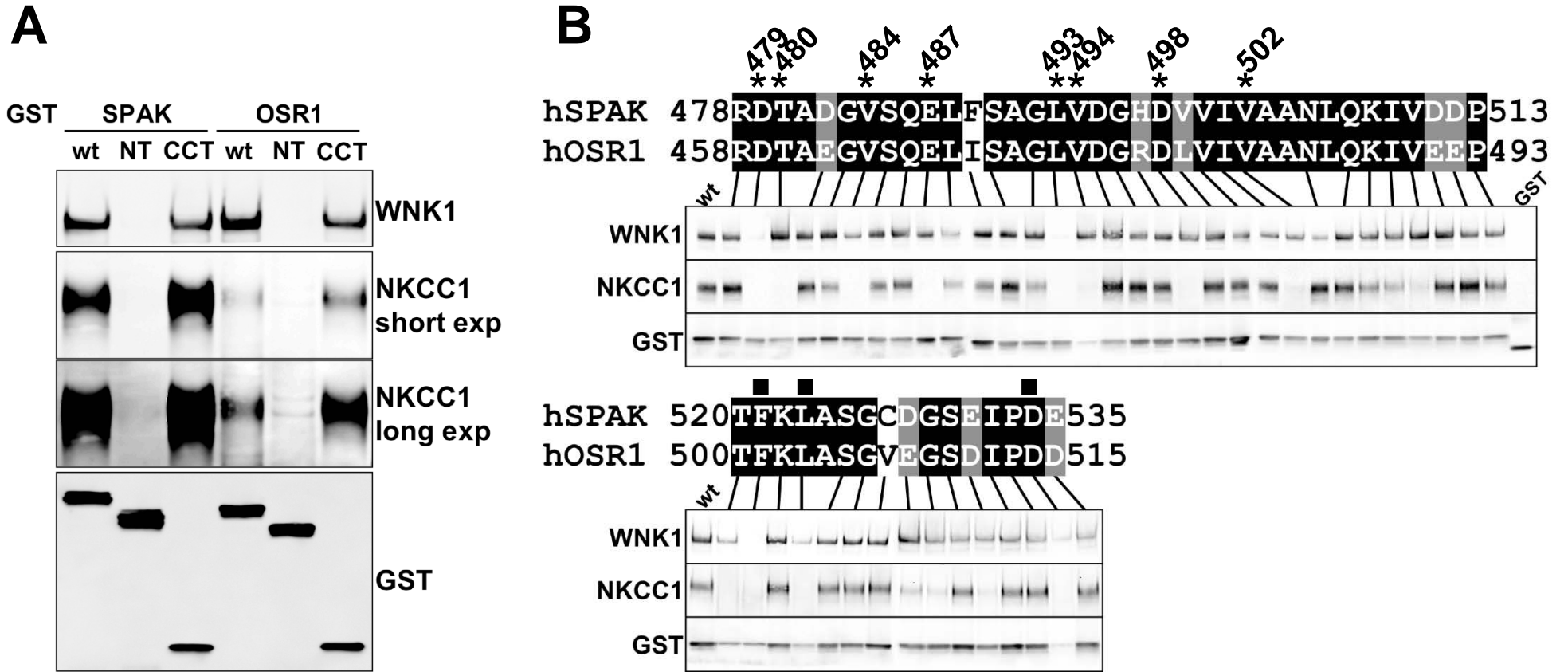
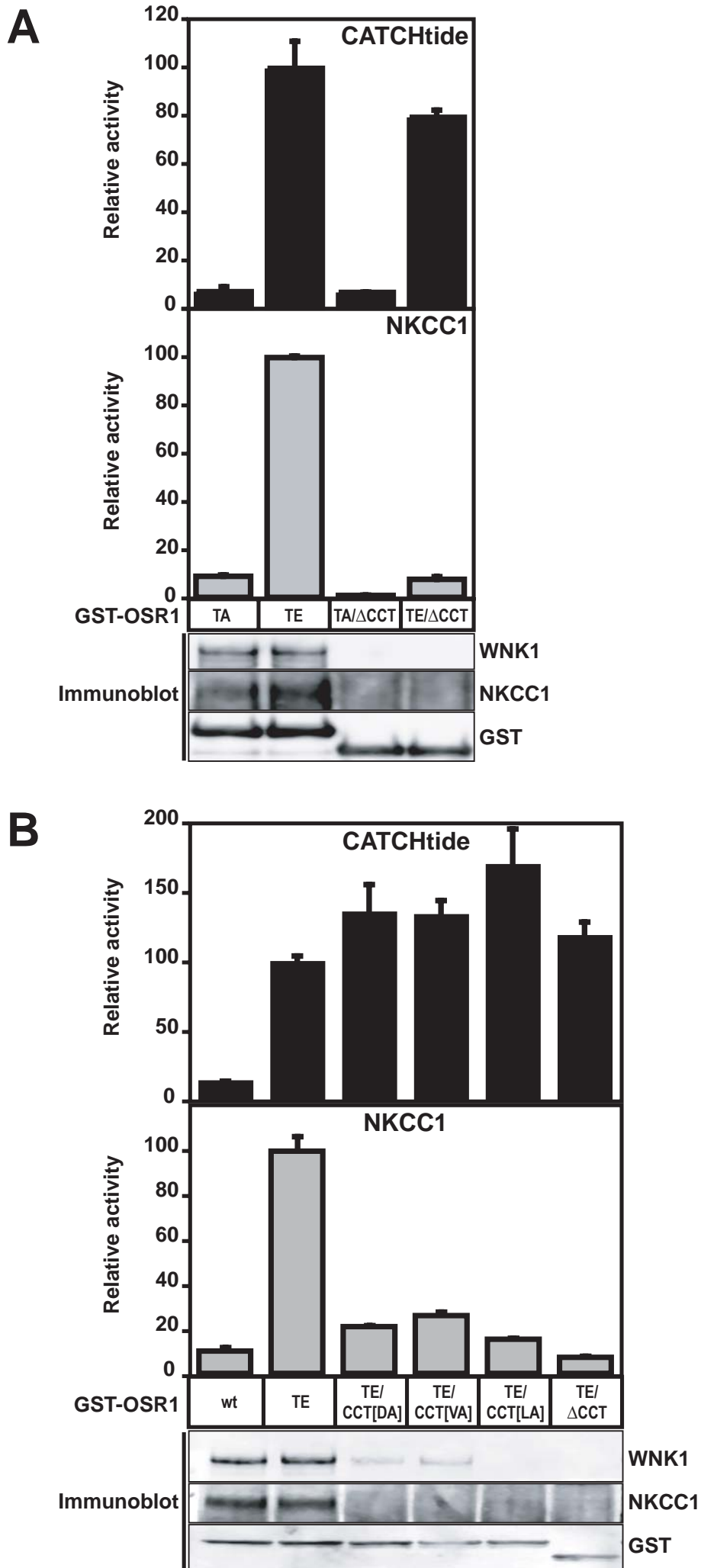
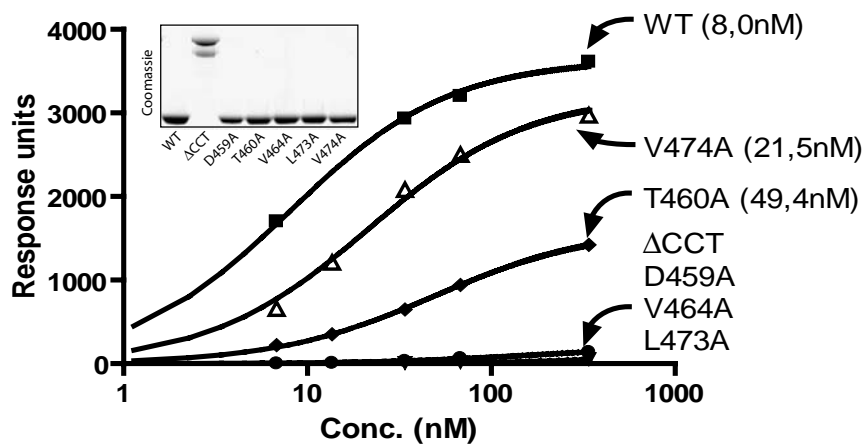


fig4

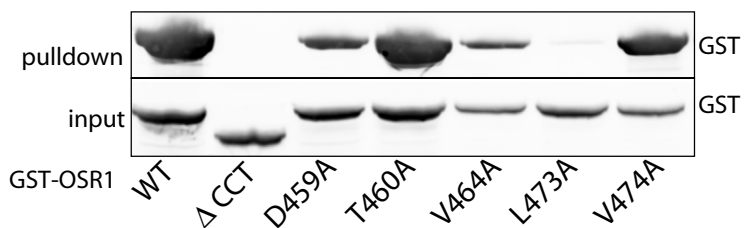


**Fig5**

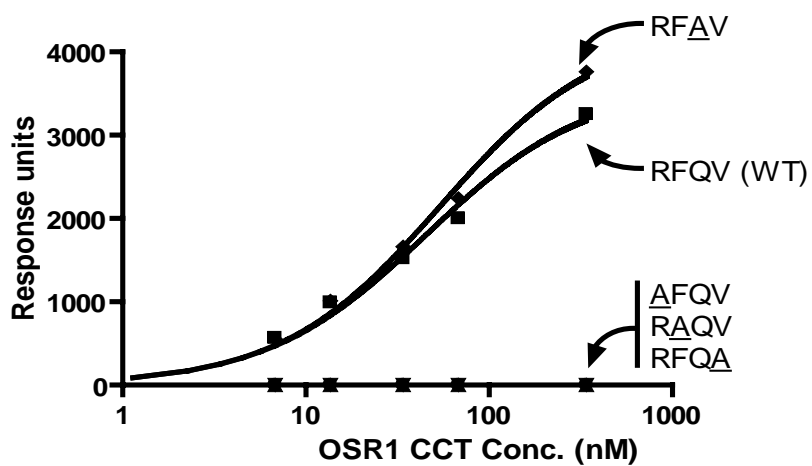
**A**



**B**



**C**



**D**

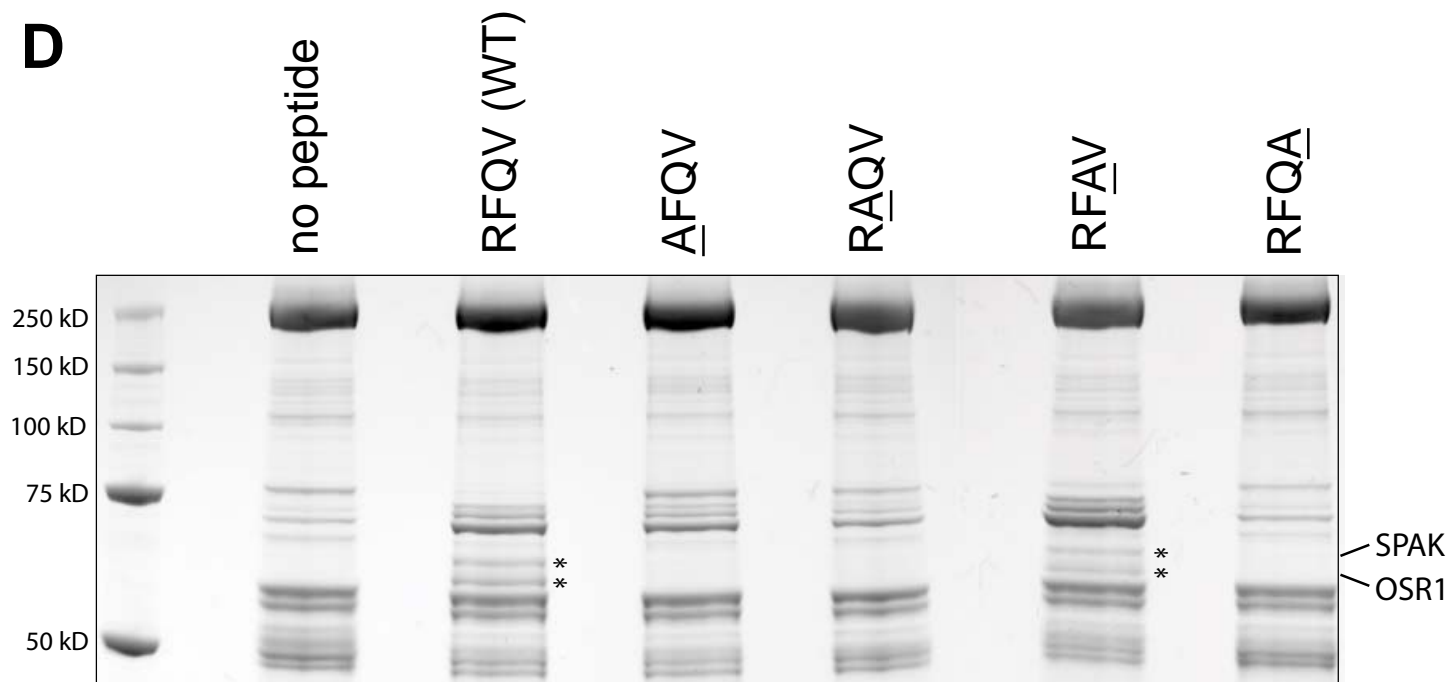
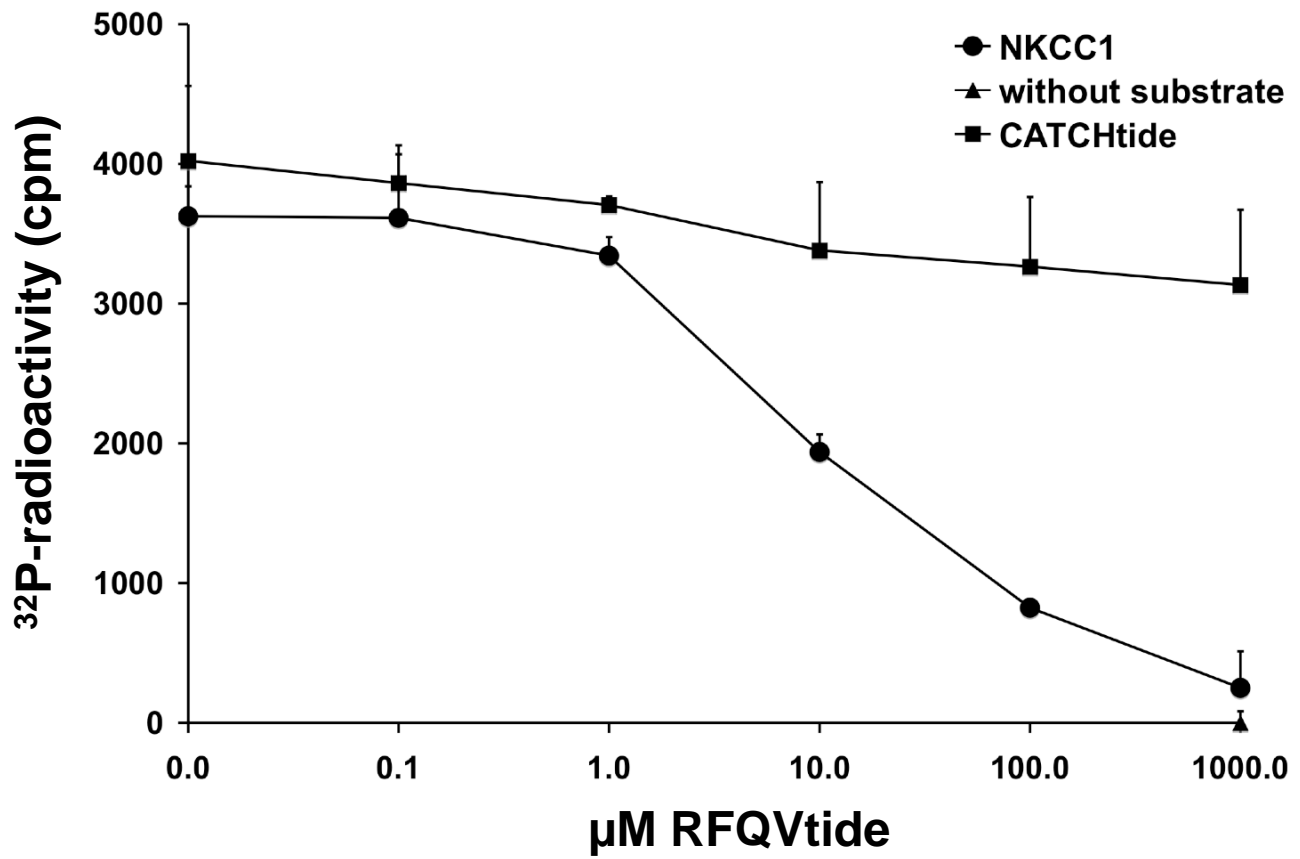


**fig6**

**A**



**B**

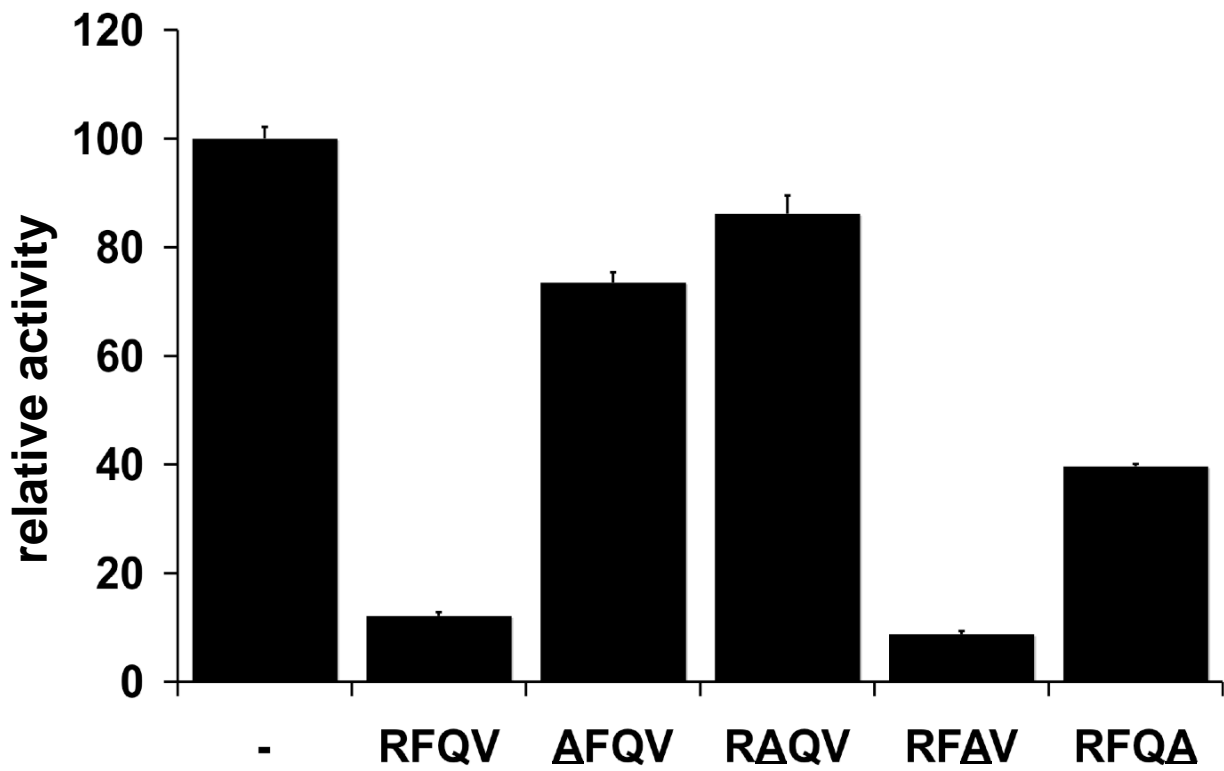


fig7

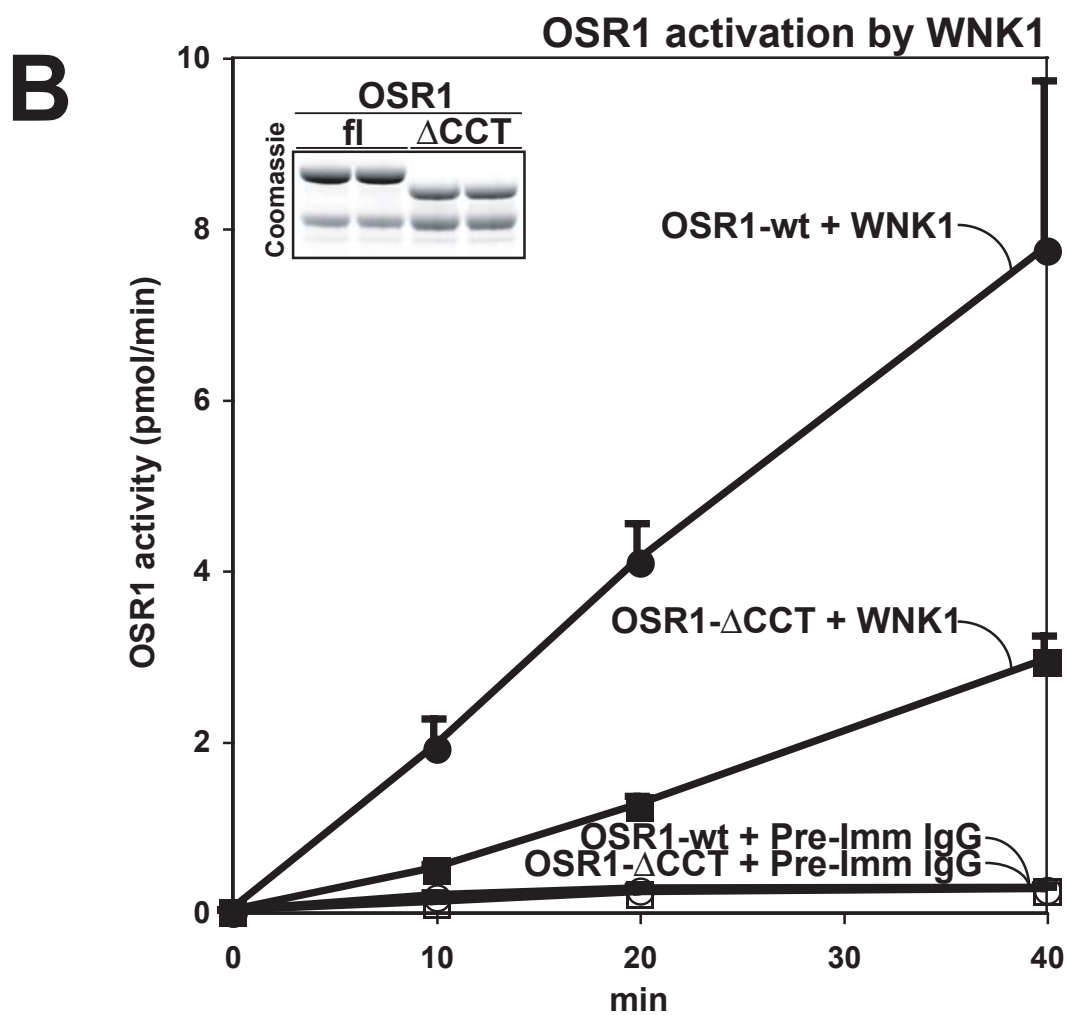
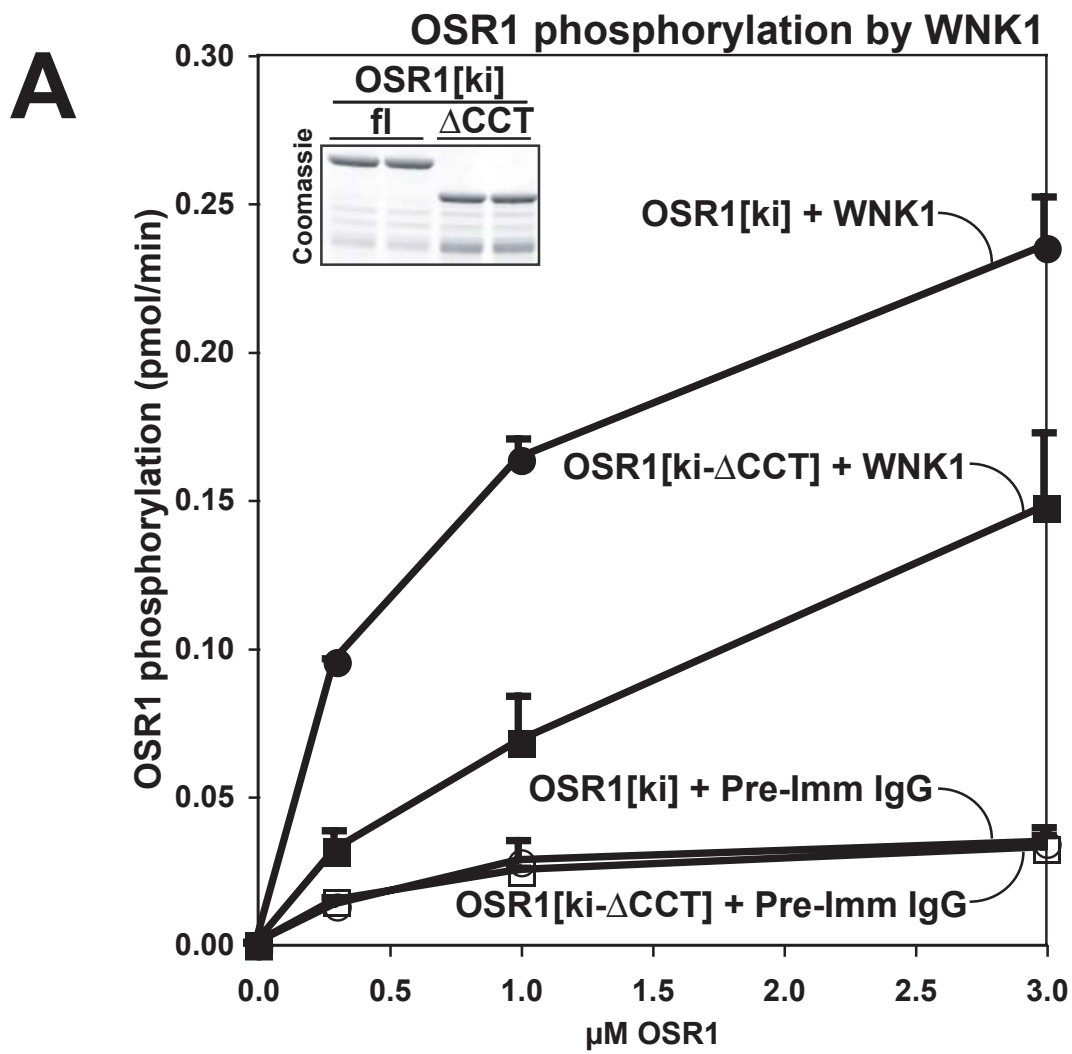


fig8